FRPRCS-11
Joaquim Barros & José Sena-Cruz (Eds)

Influence of fatigue loading and environmental conditions on the bond behavior between GFRP systems and SFRSCC substrate

P. Mendes[1], J. Barros[2], J. Sena-Cruz[3], M. Taheri[4]
[1] ISISE, University of Minho, 4800-058 Guimarães, Portugal. pmendes@civil.uminho.pt
[2] ISISE, University of Minho, 4800-058 Guimarães, Portugal. barros@civil.uminho.pt
[3] ISISE, University of Minho, 4800-058 Guimarães, Portugal. jsena@civil.uminho.pt
[4] ISISE, University of Minho, 4800-058 Guimarães, Portugal. mahsa09@gmail.com

Keywords: Bridge; GFRP; Self Compacted Steel fiber Concrete; Fatigue Tests; Aging tests.

SUMMARY
To assess the influence of fatigue loading and environmental conditions on the bond behavior between glass fiber reinforced polymer (GFRP) systems and steel fiber reinforced self-compacting concrete (SFRSCC) that are adhesively bonded, an experimental program composed of push-out tests was carried out. The following three scenarios were selected for the environmental conditions: natural conditions; wet-dry cycles; and temperature cycles. Half of the specimens were submitted to monotonic loading up to failure, and the other half were submitted to a fatigue load configuration of 1 -million cycles and then subjected to a monotonic loading up to failure. The results have shown that for the investigated environmental conditions the GFRP-SFRSCC push-out specimens never failed up to 1 million cycles. However, temperature cycles caused a considerable reduction on the stiffness and load carrying capacity in the specimens submitted to fatigue loading, while wet-dry cycles did not modify significantly the maximum shear stress transfer in the investigated connection. This paper describes in detail the experimental program, presenting and discussing the relevant results.

1. INTRODUCTION
There is always a need for innovative and durable structural load-bearing systems to accelerate construction, especially in bridges. The application of Fiber Reinforced Polymer (FRP) materials is gaining a strong momentum in structural engineering applications [1], particularly in bridges, which are typically exposed to harsh environments. Pultruded FRP shapes have the potential to replace steel sections of bridges and buildings [2]. For this purpose, Glass Fiber Reinforced Polymer (GFRP) is being dominantly used rather than other types of FRPs, such as carbon or aramid FRPs, because of its competitive cost. However, the use of composites in bridge building is still not very common, and a majority of built bridges might be considered as prototypes, Hayes et.al. [3], Keller [4] and Mendes et.al. [5].

Fiber reinforced polymer matrix composite materials have a number of advantages when compared to traditional construction materials such as steel, wood and concrete. FRPs offer excellent corrosion resistance to environmental agents, as well as the advantages of high stiffness-to-weight and strength-to-weight ratios when compared to conventional construction materials. Other advantages of FRP include low thermal expansion, good fatigue performance and damage tolerance, non-magnetic properties, ease of transport and handling, and the potential for real time monitoring [6].

The apparent high cost of FRP compared to conventional materials has been a major unfavorable restraint for a larger acceptance of these composite materials in the industry of civil engineering.

However, a direct comparison based only on the unit price is not appropriate. When installation is included in the cost comparison, FRPs can compete with conventional materials. The lightweight of FRP reduces transportation expenses and allows some prefabrication to take place at the factory, which reduces time at the job site. If the comparisons include life cycle costs, FRP can have a significant advantage. The unique properties of FRPs, such as high corrosion resistance, make the life cycle cost lower than the one corresponding to conventional materials. In many cases, a composite structure can last much longer than one of conventional materials, thus ensuring a lower life-cycle cost, Chiu and Franco [7].

The research carried out on this paper is part of a research project for the development of permanent pedestrian bridge systems using Steel Fiber reinforced Self-Compacting Concrete (SFRSCC) decks and Glass Fiber Reinforced Polymer (GFRP) girders (see Figure 1). During the first phase of the project, the creep and the structural behavior of the pedestrian bridge were investigated [5]. Two different connections configurations between the deck and the girder were evaluated. The first using steel anchors glued to the concrete deck by an epoxy adhesive and bolted to the GFRP profiles, with the deck surfaces also glued to the GFRP girders by an epoxy adhesive (see Figure 2). The second connection was assured using adhesive alone to glue the deck and the girder. Numerical simulations were carried out to appraise the possibility of using adhesive connection only. The results showed that for the serviceability and ultimate limit states the load carrying capacity of the bridge structure is not affected by using an all-adhesive connection between the deck and the girders [5]. However, it was mentioned that further investigation should be carried out to appraise the response of the connection under extreme conditions.

Therefore, the present research focuses on the adhesively bonded deck-to-girder connection behavior, under static and fatigue loading, when exposed to temperature and wet-dry cycles. The relevant results of this research can be useful for the assessment of the performance of strengthening solutions based on the use of FRP materials bonded to concrete structures through epoxy adhesives.

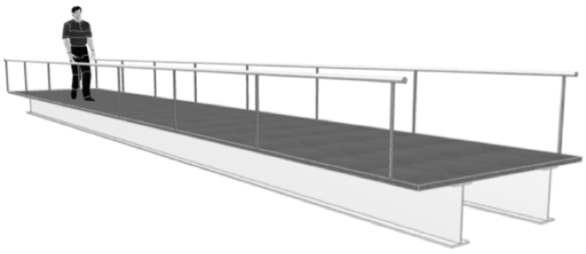

Figure 1: Bridge concept.

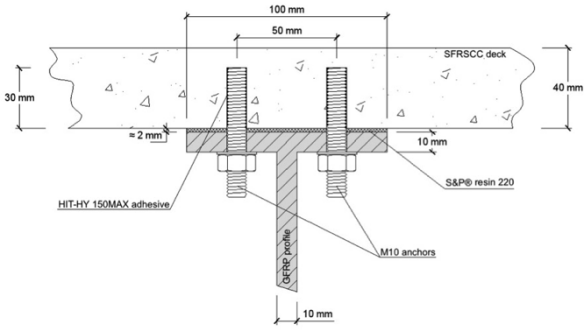

Figure 2: Connection configuration.

2. EXPERIMENTAL PROGRAM

2.1 Material properties

Table 1 shows the mixture composition of the developed SFRSCC, and Tables 2 and 3 present the relevant rheological [8] and mechanical properties of this material [9], respectively. 60 kg/m^3 of hooked ends steel fibers of 35 mm length, 0.55 mm diameter and 1100 MPa tensile strength were used. The methodology followed to formulate the SFRSCC composition is mainly based on the following three steps [8]: (i) the proportions of the constituent materials of the binder paste are defined; (ii) the proportions of each aggregate on the final granular skeleton are determined; (iii) binder paste and granular skeleton are mixed in distinct proportions until self-compacting requirements in terms of spread ability, correct flow velocity, filling ability, blockage and segregation resistance are assured, allowing the determination of the optimum paste content in concrete.

Table 1: SFRSCC mix proportion per m^3

Cement [kg]	**Limestone filler** [kg]	**Water** [kg]	**Superplasticizer** [kg]	**Fine sand** [kg]	**River sand** [kg]	**Crushed stone** [kg]	**Fibers** [kg]
380.54	353.00	140.00	7.83	237.00	710.00	590.00	60.00

Table 2: Rheological properties of the SFRSCC [8].

Parameter	**Value**
Slump flow	Diameter =80 cm T50=4 s
V-funnel	T=9 s
L-box	H2/H1=0.8

Table 3: Mechanical properties of the SFRSCC [9].

Compressive strength [MPa]	**Young's modulus** [GPa]	**Flexural tensile strength** [MPa]	$\mathbf{f_{R,1}}$ [MPa]	$\mathbf{f_{R,2}}$ [MPa]	$\mathbf{f_{R,3}}$ [MPa]	$\mathbf{f_{R,4}}$ [MPa]	$\mathbf{f_{eq,2}}$ [MPa]	$\mathbf{f_{eq,3}}$ [MPa]
47.00	34.00	10.20	9.15	11.34	9.08	7.54	9.06	9.85

The GFRP profiles were produced by the pultrusion process and are composed by E-glass fibers embedded in a polyester matrix. In accordance with several tests performed with this type of material [10], the average tensile strength in the direction parallel to the fibers is 500 MPa and the compressive strength in the same direction is 375 MPa. Moreover, two GFRP profiles were tested to evaluate the elasticity modulus, and the value of 34 GPa was obtained. The bonding agent used was the "S&P Resin 220" epoxy adhesive that, according to the supplier, presents a bending tensile strength of 30 MPa, a compressive strength of 90 MPa and bulk shear strength of 3 MPa. According to Sena et al. [11], the tensile strength, according to the ISO 527-2:1993 [12], is 21 MPa with a Young's modulus of 7.7 GPa. The glass transition temperature (Tg) is 55 °C, according to Correia et al. [10].

2.2 Test specimens, setup and instrumentation

Figure 3 shows the push-out test specimens used in the present research. The specimens consist of two concrete panels (400×250×40 mm^3) adhesively bonded to a GFRP profile. The adhesive volume in the bond between the flange of the GFRP and the SFRSCC panel is 350×100×2.5 mm^3. A needle scaler was used to ensure that the concrete laitance was removed before bonding the GFRP profiles to concrete. The surfaces of the GFRP profiles were treated using sandpaper. To ensure minimum friction between the concrete panels and the supporting steel frame (see Figure 4), rectangular plates of neoprene were used. Additionally, to prevent any suddenly failure of the specimen, a passive confinement system was used (see Figure 4).

A total of 18 specimens were tested. The specimens were divided into three series according to the type of exposure used: reference exposure, temperature cycles, and wet-dry cycles. The first character in the specimen ID indicates the series number (R for reference, T for temperature cycles and WD for wet-dry cycles), the middle character specifies the loading type, such as S for static, F for fatigue and PF for post-fatigue, and the last character gives the specimen number. As an example, R_S1 stands for the static loading for the reference specimen number one.

The push-out specimens were tested with a vertical pushing load, as shown in Figure 4. The monotonic load and the fatigue load were applied using a 500 kN servo-hydraulic actuator incorporating a load cell of 500 kN.

To measure the bond slip between the flanges of the GFRP profile and SFRSCC, five LVDTs (LVDT 1 to 5) with a stroke of 5 mm were placed with a regular pattern in four different locations along the

bond length. The supports used to hold these LVDTs are perfectly aligned in the horizontal plan. Two LVDTs of 10 mm stroke were used (LVDT 6 and 7) to measure the relative horizontal movement of the concrete panels.

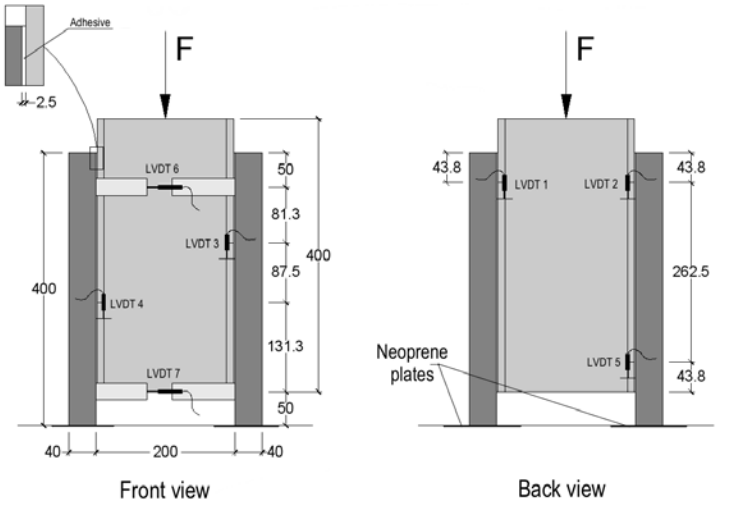

Figure 3: Tested specimens (dimensions in mm).

Figure 4: Test apparatus.

2.3 Exposure environments

The connection system proposed in the present paper is intended to be used in a full-scale composite pedestrian bridge to be installed in the north of the Portuguese territory. Thus, to ensure a long service live and guarantee its proper functioning, with minimal maintenance, is essential to estimate the long-term behavior of such connection under different environmental conditions. Therefore, the exposure conditions chosen for this research were based on the characteristics of the actual environment to which the bridge structure will be exposed.

The north of the Portuguese territory features the Mediterranean climate, with warm, dry summers and mild, rainy winters. Summers are typically sunny with average temperatures between 14 °C and 28 °C, but can rise to as high as 36 °C during occasional heat waves. During such heat waves the humidity can reach 95 %, however, during summer, the average relative humidity is 80 %. Winter temperatures typically range between 4 °C during morning and 14 °C in the afternoon but rarely drop below 0 °C at night [13].

Based on such conditions, to different types of exposure were considered for the present research: alternate wet-dry cycles and temperature variation cycles. In addition, one group of specimens was kept in the laboratory as control specimens. Details of specimens tested under various exposure regimes are shown in Table 4.

Table 4: Specimens and test programme

Exposure regime	Duration	No. of specimens
Wet-dry	100 cycles (one cycle = 1 day)	6
Temperature cycle	100 cycles (one cycle = 4 hours)	6
Control	3 months	6

In the alternate wet-dry exposure, each cycle consisted of complete immersion of the specimens in 3 % NaCl solution for 12 hours followed by drying in air another 12 hours. The NaCl solution was used to simulate the worst-case scenario, where the structure is located near the shore. For such cycles two separate containers were used, each one equipped with a water pump programed to pump the water for one container to another in each 12 hours. The water was kept at 20 ºC using a thermostat during

immersion, and the air was kept approximately at 25 ºC during the drying period using a thermo ventilator. Two small pumps were installed in each container to circle the water, avoiding the sedimentation of the salt as well as the water impurities.

A total of 100 cycles were repeated with the described conditions. The amount of salt in the water was decided from the stipulated guidelines provided by ASTM B 117-85 for salt spray (fog) testing. The pH of the solution was found between 7.5 and 8.0.

In the temperature cycle exposure, a climatic chamber was used with temperature and humidity regulation capability. A typical cycle of temperature variation with time used in the tests is shown in Figure 5, i.e. six cycles a day with maximum and minimum temperatures of 60 ºC and -10 ºC, respectively. The specimens were exposed to a total of 100 cycles, with a RH of 80 % during positive temperatures, and approximately 10 % during negative temperatures.

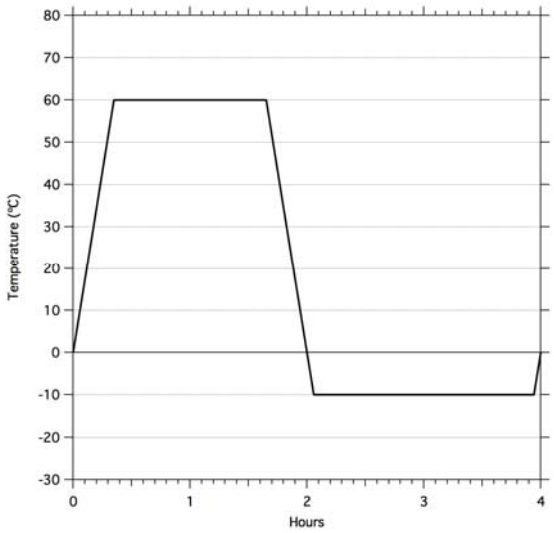

Figure 5: Temperature variation in the temperature cycle exposure.

2.4 Test procedures

To develop an all-adhesive connection for use in pedestrian bridge systems, it is essential to analyze the bond behavior under different exposure and loading conditions. Thus, three different load scenarios were used: static load, fatigue load and post-fatigue static load.

The static load allows the determination of the bond-slip relationship, as well as the ultimate bond strength. The fatigue loading allows the assessment of the connection behavior at long-term. And lastly, the post-fatigue static load allowed the evaluation of the changes in the stiffness and bonding capabilities after fatigue loading.

The static load and the post-fatigue static load tests were carried under displacement control mode. The static load was applied monotonically until failure. The displacement rate was kept at a rate of 0.2 mm/min, and was controlled by the internal LVDT of the actuator. The fatigue load was determined based on previous tests and numerical simulations of the bridge structure [5], which allowed the determination of the maximum shear stress in the GFRP-concrete connection for the serviceability limit states. Therefore, to determine the load to obtain the equivalent shear stress, one reference specimen was monitored with strain gauges under static load. The results obtained allowed the determination of the fatigue load range. Hence, the fatigue tests were carried out at maximum and minimum stress ratios of S_{max} (F_{max}/F_{ult}) = 0.48 and S_{min} (F_{min}/F_{ult}) = 0.14. All tests ran at a load ratio R (F_{min}/F_{max}) = 0.28. Therefore, the specimens were first loaded statically up to 90 kN, and then the fatigue load was applied between 40 kN and 140 kN, corresponding to a variation of ±50 kN. All specimens were subjected to 1 million sinusoidal load cycles at a frequency of 2 Hz, and the sinusoidal

loading was force controlled. The cycle readings were taken at the following rate: every 1000 cycles 10 cycles were recorded. Note that in the subsequent sections the results showed are for the representative push-out specimen from the three specimens tested.

3. TEST RESULTS AND DISCUSSION

3.1 Monotonic tests

Figure 6 shows the typical load-slip curves for the three different environmental exposures. The control exposure (R series) exhibited the highest peak load, reaching approximately 315 kN, with a loaded end slip of 69 μm. The results from temperature cycles exposure (T series) reveal that, when compared to the ones of the control exposure, the peak load and the loaded end slip decreased significantly, reaching 183 kN and 42 μm, respectively, presenting reduction of 41 % in terms of load carrying capacity. This behavior was a consequence of the stress cycles imposed by the temperature cycles. Also, the temperature cycles exceeded the Tg (56ºC), which, according to Moussa et al [14], has a negative impact the bond strength and stiffness.

Considering the wet-dry cycles (WD series), the results show an increase of the specimen stiffness up to a load of 150 kN, then the stiffness remained identical to the control exposure up to a load of 250 kN, followed by a decrease in the bond stiffness. The peak load also decreased slightly, reaching 296 kN with a loaded end slip of 48 μm, corresponding to a reduction of approximately 6 % and 30 %, respectively, when compared to the control exposure. The increase of the initial stiffness for the WD series could be explained by the less aggressive and best curing conditions provided by the WD exposure, i.e., the temperature ranged between 20 ºC to 25 ºC, which lead to a slowly and gradual curing of the adhesive. Due to this stiffer behavior of the connection system, it is natural that when damage initiates, its effect is more pronounced, not only in terms of stiffness but also in terms of ultimate load, due to a more abrupt release of the energy accumulated in the constituent materials and bond systems, which justifies the behavior of the last phase of the WD series.

Figure 7 presents the failure modes of the specimens after the monotonic tests. The failure occurred only in one of the bonded flanges of the GFRP profile. Although all specimens failed by debonding, the concrete layer peeled off varied with the type of exposure, and thus affecting the bond stiffness and strength. It is noticeable that at the loaded-end, in the T and WD series, small portions of adhesive remained bonded to the concrete, meaning that cohesive failure occurred. This small portions of cohesive failure denoted that, under such weathering conditions, the adhesive tends to be the weakest link.

In the control specimens the debonding was uniform and the concrete layer peeled off was evenly thick (Figure 7a). This figure also shows the presence of some aggregates in the concrete layer peeled off, denoting the stiffness of the connection.

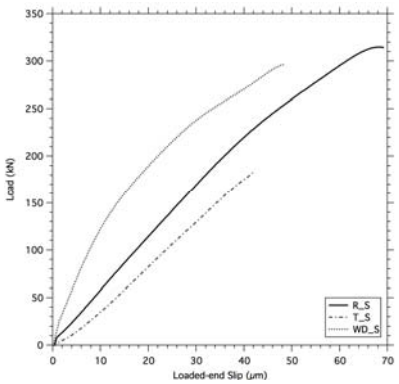

Figure 6: Load-slip curves of monotonic tests.

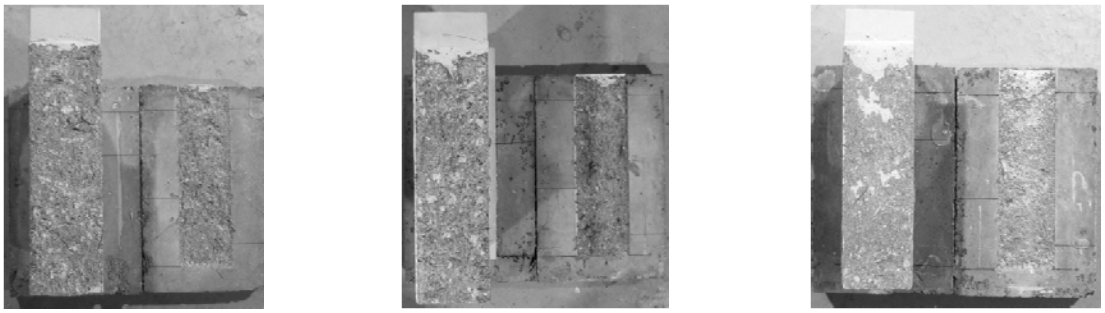

(a) (b) (c)

Figure 7: Failure modes in the monotonic tests of series: (a) R; (b) T, and (c) WD.

3.2 Fatigue behavior

In Figure 8, the loaded end slip *versus* number of cycles at both the maximum and the minimum load levels are plotted for each exposure condition. The shape of the curves is generally similar among the different exposure conditions. Initially, a significant increase of slip is observed up to the 100,000th cycle, which is then followed by a mild growth period where the slip increased slowly until the last cycle. This clearly indicates the continuous degradation of the bond interface during the fatigue load cycles.

Closer scrutiny reveals some significant differences between the three exposure conditions. In the case of the R series, the results show that the bond degradation was smaller than the one registered in the others exposures, i.e. the slip amplitude varied between 14 and 16.5 μm (see Figure 9). Another important aspect is the variation of the slip amplitude, which in the case of the R series remained nearly constant during the fatigue loading, indicating a steady energy dissipation due to progressive growth of micro-cracking. In the case of T series, the slip amplitude remained almost constant during the fatigue loading, however is much larger than the slip amplitude in the specimens subjected to the control exposure, indicating a greater dissipation of energy due to a more intense formation of micro cracks in the adhesive. Thus, in T_F series the slip amplitude varied between 26.5 and 30 μm, which correspond to an increase of approximately 86 % when compared to R series. Lastly, the slip amplitude also remained constant during the fatigue loading in the WD series, however developing a greater amplitude of slip than the specimens subjected to control exposure. In the WD_F series the slip amplitude varied between 16,5 and 20 μm, corresponding to an increase of 20 % when compared to R series. Thus, the slip amplitude in the T and WD series is significantly larger, which indicates a less stiff and durable bond, being the T series the one that showed the grater degradation.

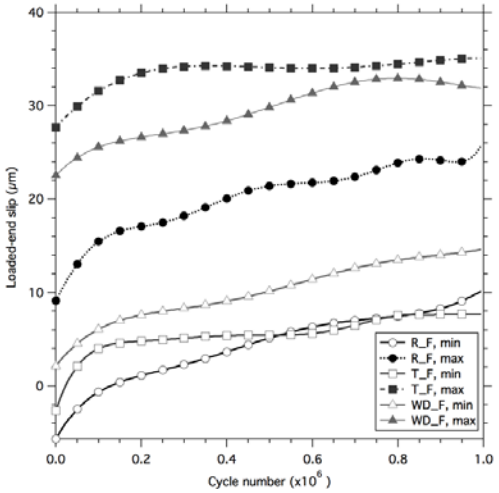

Figure 8: Slip vs. number of cycles of the three different exposures under fatigue loading.

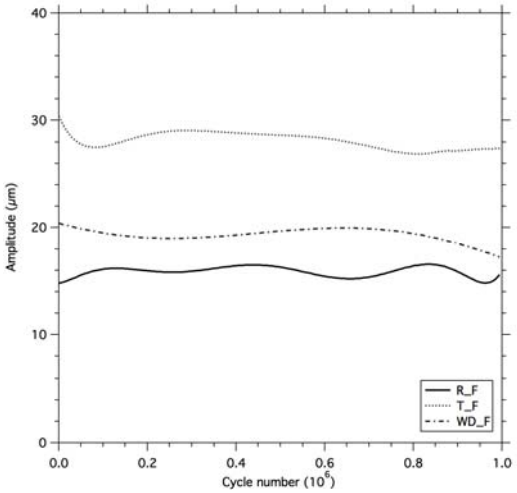

Figure 9: Slip amplitude for the three different exposures.

3.3 Post-fatigue monotonic behavior

After the fatigue tests, all specimens were loaded monotonically up to failure, being the results presented in Figure 10. Due to the fatigue loading effect, the specimens showed a significant increase in the bond stiffness up to a load range between 50 and 100 kN. This phenomenon can be explained by the densest and more compact connection resulted from the fatigue load, promoting a more homogeneous microstructure of the adhesive. Subsequently the specimen starts to reach inexperienced load levels (fatigue loading between 40 and 140 kN), causing a reduction in the bond stiffness, which remains identical to the results from the monotonic tests.
Thus, the control exposure (R series) reached a peak load of approximately 310 kN, with a loaded end slip of 32 μm, presenting reduction of 1 % and 53 %, respectively, when compared to the corresponding results registered in the homologous specimens subjected to control exposure and tested in monotonic load conditions. Hence, the fatigue load reduced the ductility of the bond, since the strength remained identical for half of the bond slip.

The specimens subjected to temperature cycles (T series), after the initial "elastic" phase (that started at about 90 kN) presented a softer response than the specimens of the R series. The lower bond stiffness is in agreement with the results from the fatigue behavior for the same specimen, where the slip amplitude was also larger when compared to other series.

The specimens of the WD series, after the initial "elastic" phase (that started at about 50 kN), developed a stiffer behavior than the specimens of the R series. The peak load reached 315 kN, at a loaded end slip of 30 μm, which correspond to an increase of 6 % and a reduction of 37% when compared to the results registered in the specimens subjected to wet-dry cycles and tested under monotonic loading conditions. This behavior is also in agreement with the results obtained in the fatigue tests, where the slip amplitude was smaller than the one determined in the specimen of T series, which justifies the stiffer bond response of the specimens submitted to WD conditions.

All specimens registered a stiffest peak behavior, when compared to the homologous specimens. This behavior is consequence of the test setup, which in the case of the present monotonic tests was slightly different. Thus, in the present test setup the confinement system (see Figure 4) was kept tighter, to prevent any brittle failure due to the fatigue history of the specimen, leaving only 1 mm of clearance between the steel member and the concrete plate. Thus, when the passive confinement starts to become active, the system becomes stiffer, leading to a stiffest peak behavior.

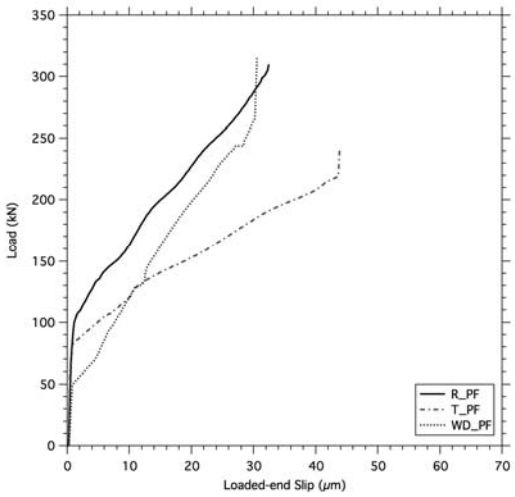

Figure 10: Load slip curves of the post-fatigue tests.

Figure 11 presents the failure modes observed in the specimens that after have been subjected to fatigue loading, were tested under monotonic loading up to failure. Once again, the failure occurred only in one of the bonded flanges of the GFRP profile. Moreover, these failure modes were very

similar to those registered in the monotonic tests, which means that the failure mode was not affected by the fatigue loading.

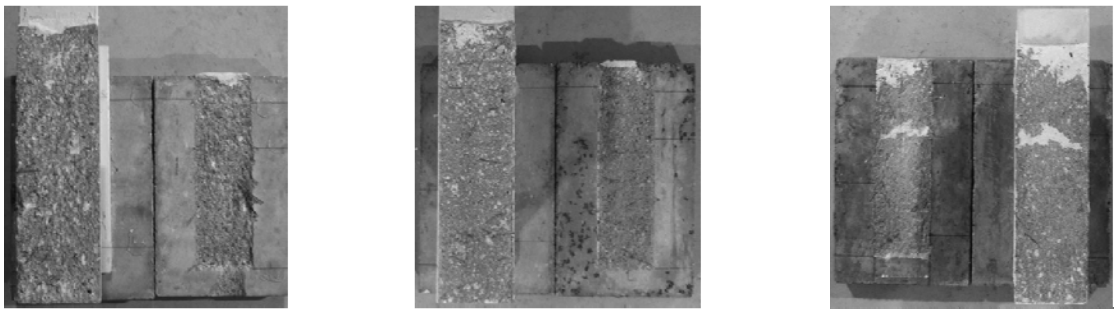

(a) (b) (c)

Figure 11: Failure modes for the post-fatigue monotonic tests in specimens of series: (a) R; (b) T, and (c) WD.

5. CONCLUSIONS

The performance under static, fatigue and aggressive exposure of the proposed adhesive joints was investigated experimentally. Based on the results of the investigations presented in this paper, the following conclusions can be pointed out:

- The results from the monotonic tests evidenced that when the connection is exposed to the temperature cycles (T series) a reduction of 41 % in the peak load was obtained, when compared to the control exposure, indicating that the detrimental effect of the temperature cycles should be considered on the design evaluation of the long term performance of this type of connection.
- The failure modes for the monotonic tests showed that all specimens failed by debonding. However, the area of the concrete layer peeled off has varied with the type of exposure, and thus affecting the bond stiffness and strength of the connection. For the T and WD series, in some portions of the bonded area, cohesive failure of the adhesive occurred due to the aggressive exposure, being more pronounced in the WD series.
- The fatigue behavior showed a slightly continuous degradation of the bond interface during the fatigue load cycles. These results also revealed that during the fatigue loading the specimens from the WD series presented a less stiff response, since the slip amplitude was larger than those of the reference specimens. Moreover, from the maximum and the minimum slip curves, it is noticeable that the stiffness remained constant during the fatigue loading for the three series. After 1 million cycles, the specimens did not display any visible damage.
- The post-fatigue monotonic behavior was affected by the fatigue loading, i.e., in terms of initial stiffness the fatigue loading had a favorable effect of increasing significantly bond stiffness up to a load interval between 50 and 100 kN. Then, when the monotonic load level applied to the specimen exceeded the maximum load level the specimen has experienced in the fatigue loading process, a significant reduction in the bond stiffness occurs, becoming identical to the stiffness registered in the monotonic tests.

ACKNOWLEDGMENTS

This research is part of the research project funded by ADI co-financing FEDER by POFC - COMPETE of QREN No 3456 – PONTALUMIS Development of a prototype of a pedestrian bridge in GFRP-ECC concept, involving the Company ALTO – Perfis Pultrudidos, Lda., the ISISE/University of Minho and the ICIST/Technical University of Lisbon. The first author wish to acknowledge the research grant under this project. The authors also wish to acknowledge the Civitest Company for the conception and development of the steel fiber reinforced self-compacting concrete used in this work, to Secil and S&P Clever Reinforcement Ibérica, Lda. for the supplied materials and technical support.

REFERENCES

[1] Bank LC. Composites for Construction: structural design wiyh FRP materials. Polymer. Hoboken, NJ: JOHN WILEY & SONS; 2006.
[2] Bakis CE, Bank LC, Asce F, Brown VL, Asce M, Cosenza E, et al. Fiber-Reinforced Polymer Composites for Construction — State-of-the-Art Review. Journal of Composites for Construction. 2002;6(2):73–87.
[3] Hayes MD, Lesko JJ, Haramis J, Cousins TE, Gomez J, Masarelli P. Laboratory and Field Testing of Composite Bridge Superstructure. Journal of Composites for Construction. ASCE; 2000;4(3):120–8.
[4] Keller T. Use of fibre reinforced polymers in bridge construction. International Association for Bridge and Structural Engineering; 2003.
[5] Mendes PJD, Barros JAO, Sena-Cruz JM, Taheri M. Development of a pedestrian bridge with GFRP profiles and fiber reinforced self-compacting concrete deck. Composite Structures. 2011 Oct;93(11):2969–82.
[6] Hejll A, Täljsten B, Motavalli M. Large scale hybrid FRP composite girders for use in bridge structures—theory, test and field application. Composites Part B: Engineering. 2005 Dec;36(8):573–85.
[7] Chiu A, Franco RJ. FRP line pipe for oil and gas production. Mod Plast 1990;June:54–60.
[8] Pereira ENB. "Steel fibre reinforced self-compacting concrete: from material to mechanical behaviour". Dissertation for pedagogical and scientific aptitude proofs. Department Civil Engineering, University of Minho; 2006. 188 pp. <http://www.civil.uminho.pt/composites>.
[9] EFNARC, Specification and Guidelines for Self-Compacting Concrete (2002), ISBN, 0 9539733 4 4, 32 pp.
[10] Correia JR. Glass fibre reinforced polymer (GFRP) pultruded profiles. Structural behaviour of GFRP-concrete hybrid beams [Internet]. Instituto Superior Técnico; 2004 [cited 2012 Aug 24]. Available from: https://dspace.ist.utl.pt/bitstream/2295/61623/1/Programa-EQC
[11] Sena-Cruz, J.M.; Michels, J.; Czaderski, C.; Motavalli, M.; Castro, F. (2012) "Mechanical behavior of epoxy adhesives cured at high temperatures", Report no. 880163, Empa, Swiss Federal Laboratories for Materials Science and Technology, Suíça, 40 pp.
[12] ISO 527-2:1993. "Plastics — Determination of tensile properties — Part 2: Test conditions for moulding and extrusion plastics." International Organization for Standardization – ISO, Genève, 8 pp.
[13] Meteorologia IP. Boletim Climatológico Anual - 2011 Factos e Fenómenos Climáticos Relevantes em 2011. Lisbon; 2011.
[14] Moussa O, Vassilopoulos AP, De Castro J, Keller T. Early-age tensile properties of structural epoxy adhesives subjected to low-temperature curing. International Journal of Adhesion and Adhesives [Internet]. Elsevier; 2012 Jun [cited 2012 Dec 17];35:9–16. Available from: http://linkinghub.elsevier.com/retrieve/pii/S0143749612000243